Quaternary International 621 (2022) 16–25

Contents lists available at ScienceDirect

Quaternary International

journal homepage: www.elsevier.com/locate/quaint

Impact of extreme wet and dry years on the persistence of *Microcystis* harmful algal blooms in San Francisco Estuary

P.W. Lehman [a,*], T. Kurobe [b], S.J. Teh [b]

[a] California Department of Water Resources, 3500 Industrial Blvd, West Sacramento, CA, 95691, USA
[b] Department of Anatomy, Physiology and Cell Biology, School of Veterinary Medicine, University of California, Davis, CA, 95616, USA

ARTICLE INFO

Keywords:
Microcystis
Drought
Temperature
Streamflow
Climate

ABSTRACT

Cyanobacteria harmful algal blooms (CHABs) became a concern in the upper San Francisco Estuary, California beginning in 1999, when yearly blooms of *Microcystis* began in the Delta region. Subsequent research identified that the increase in the magnitude, duration and toxicity of *Microcystis* blooms was associated with drought related conditions of elevated water temperature and low streamflow. However, the impact of extreme conditions on the resilience of the bloom was unknown. The 2014 and 2017 water years provided a unique opportunity to determine the effect of climatic "whiplash" produced by the occurrence of extreme wet conditions following extreme dry conditions on the *Microcystis* bloom. We hypothesized that the period of record wet conditions in 2017 (1906-2018) would eliminate the *Microcystis* bloom for that year and perhaps revert the estuary phytoplankton community back to pre-bloom conditions due to extreme flushing, despite the increase in magnitude and spatial and temporal distribution of the *Microcystis* bloom during the 2014 extreme dry year. Field sampling was conducted at 2-week or 4-week intervals between July and November at stations throughout the Delta for both years and included a suite of physical, chemical and biological factors. Using PRIMER-e DISTLM, we determined that retention time in the upper estuary and water temperature were key environmental correlates with the *Microcystis* bloom amplitude and in regression models described 58-78% of the variation of the bloom surface biovolume or subsurface abundance. The period of record high streamflow in 2017 was not enough to eliminate the *Microcystis* bloom. However, the bloom was small in 2017, with a low abundance, late initiation, short duration, narrow distribution and low toxin production. Warm water temperature enabled the bloom to flower in late summer despite streamflow many times those measured previously. In addition, although conditions early in the summer of 2017 favored diatoms, the summer was characterized by an abundance of other non-*Microcystis* cyanobacteria. We conclude that once established, *Microcystis* is likely to be resistant to extreme wet conditions, as long as water temperature and other key water quality conditions are favorable.

1. Introduction

Microcystis has increased worldwide and its increase is partially attributed to the increase in drought conditions caused by climate change because *Microcystis* thrives in regions with elevated water temperature, decreased flushing time, water column stratification and accumulation of nutrients associated with drought (Harke et al., 2016; Paerl and Otten, 2013). Climate change is predicted to increase the frequency and intensity of extreme drought and flood events worldwide (IPCC, 2014). Increased frequency of these extreme events will lead to rapid shifts from extreme dry to extreme wet conditions or climatic "whiplash" in California (Swain et al., 2018) and it is unknown how these rapid shifts in extreme environmental conditions will impact biological communities, including cyanobacteria harmful algal blooms (CHABs). *Microcystis* is currently the most common freshwater CHAB worldwide (Harke et al., 2016) and has expanded into estuarine habitats including the Chesapeake Bay, San Francisco Bay and the Neuse River Estuaries in the United States; the Swan River Estuary in Australia; the Los Platos Estuary in Brazil; and the Guadiana River Estuary in both Spain and Portugal (Sellner et al., 1988; Yunes et al., 1996; Rocha et al., 2002; Robson and Hamilton, 2003; Lehman et al., 2005). In addition, transport of *Microcystis* from freshwater and estuarine environments seaward can affect the survival and toxicity of marine species along the coastal ocean (Miller et al., 2010).

* Corresponding author.
E-mail address: Peggy.Lehman@water.ca.gov (P.W. Lehman).

https://doi.org/10.1016/j.quaint.2019.12.003
Received 17 June 2019; Received in revised form 10 October 2019; Accepted 2 December 2019
Available online 7 January 2020

Microcystis spp. (*Microcystis*) has bloomed during the summer and fall in upper San Francisco Estuary (USFE) since 1999 (Lehman et al., 2017). The blooms are an environmental threat to estuarine species in USFE where it has been demonstrated that these blooms affect the health and survival of fish (Acuña et al., 2012a,b; Kurobe et al., 2018a,b), zooplankton (Ger et al., 2009, 2010), and the composition of phytoplankton and bacterial communities (Lehman et al., 2010; Kurobe et al., 2018a). Blooms vary more with wet and dry conditions than with nutrient concentration in this nutrient replete estuary (Lehman et al., 2008, 2017), even though *Microcystis* increases linearly with the percentage of ammonium in the total nitrogen pool (Lehman et al., 2015). The 2014 water year was one of the driest years on record in USFE (http://cdec.water.ca.gov/cgi-progs/iodir/WSHIST) and was accompanied by a *Microcystis* bloom that was 13–76% larger than precious blooms in dry or wet years, respectively (Lehman et al., 2017). Given the large *Microcystis* bloom during the 2014 drought year, it is expected that *Microcystis* will increase with the increased frequency of drought conditions predicted to occur in California due to climate change (Dettinger et al., 2016; Jones, 2015; Cayan et al., 2009). However, it is unclear how *Microcystis* blooms and the associated primary producer community (phytoplankton and cyanobacteria) will vary with alternating wet and dry conditions or climatic "whiplash" (Swain et al., 2018). The potential removal of *Microcystis* and return to pre-bloom conditions during extreme wet conditions was suggested by the near replacement of *Microcystis* by *Aphanizomenon* spp. in 2011 (Mioni et al., 2011), which was a year with comparatively high streamflow in USFE (Dettinger et al., 2016; http://cdec.water.ca.gov/cgi-progs/iodir/WSHIST).

We hypothesized that *Microcystis* would respond rapidly and on a yearly basis to changes in extreme wet and dry conditions, and specifically that a *Microcystis* bloom would not occur in an extreme wet year, even after an extreme drought year with a large *Microcystis* bloom as a seed source. To test this hypothesis, we compared the magnitude and toxicity of *Microcystis* blooms during the extreme drought of 2014 and the extreme flood of 2017. The water year 2014 was the 3rd and 4th driest year and the water year 2017 was the 1st and 2nd wettest year on recorded since 1906 for the Sacramento and San Joaquin River watersheds, respectively (http://cdec.water.ca.gov/cgi-progs/iodir/WSHIST). These two years also occurred within the climatic "whiplash" in California caused by the rapid change from extreme drought between 2012 and 2016 to extreme flood in 2017 (Swain et al., 2018). Comparisons were made with physical, chemical and biological data collected at 2 to 4-week intervals between July and November, at 14 stations throughout USFE in 2014 and 2017. Environmental conditions and primary producer communities associated with these extreme wet and dry years were also used to determine their potential impact on the *Microcystis* bloom.

2. Site description

San Francisco Estuary, located in central California, is the largest estuary on the west coast of North America. The USFE is comprised of an inland delta (Delta) of 2,990 km^2 with 1,100 km of waterways, which is bounded by the Sacramento River on the north and the San Joaquin River on the south (Fig. 1). The Delta extends upstream to the head of the tide at Freeport on the Sacramento River and Vernalis on the San Joaquin River. The location where these two major rivers converge near Antioch is called the confluence and water flows (outflow; Fig. 2) past the confluence into a chain of downstream marine bays - Suisun, San

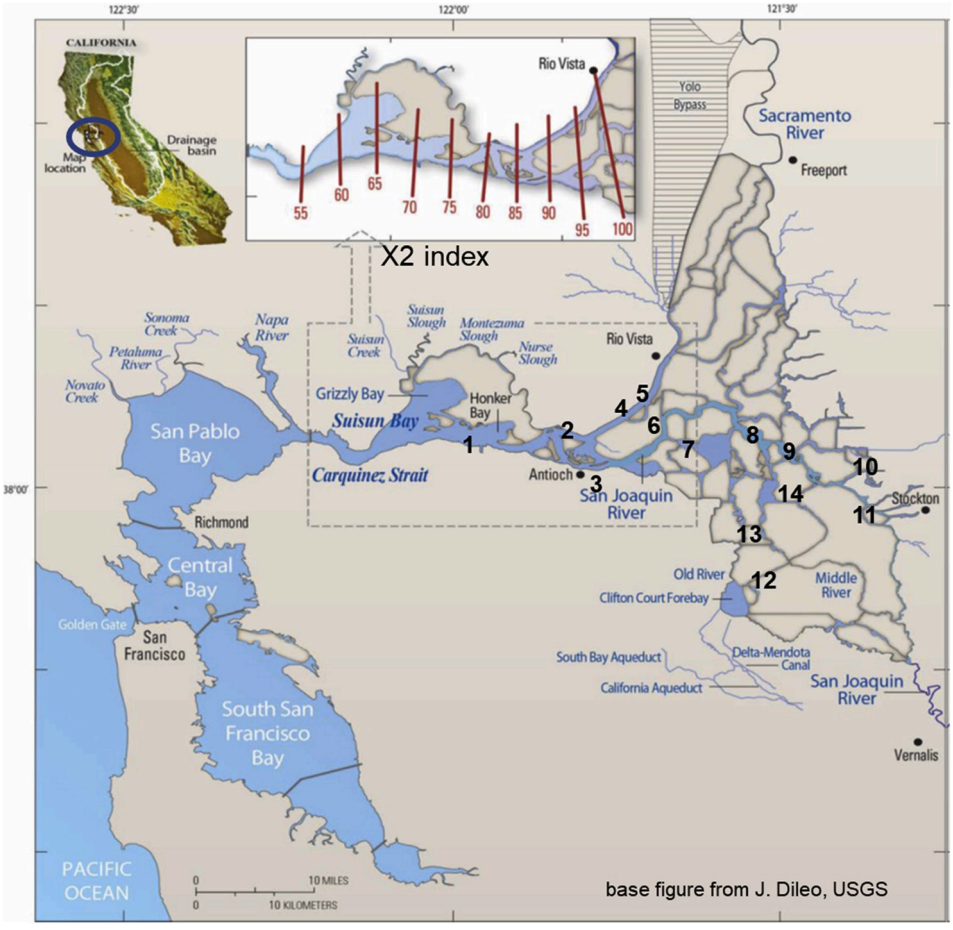

Fig. 1. Map of the upper San Francisco Estuary and stations sampled in 2014 and/or 2017. Insets indicate the location of the estuary in California and locations of the X2 index (km), the distance inland from the Pacific Ocean where bottom salinity is 2.

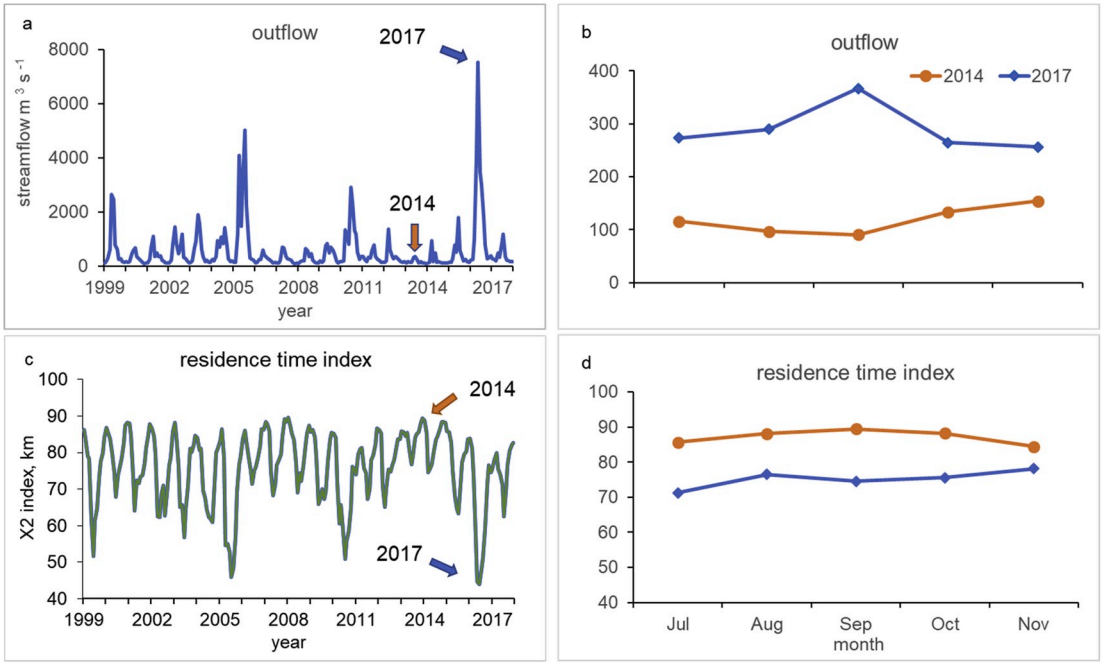

Fig. 2. Monthly average outflow (a) and the residence time index X2 (c) measured for the upper estuary between 1999 and 2017 and monthly average outflow (b) and the residence time index X2 (d) measured during the *Microcystis* bloom season between July and November for 2014 (circle) and 2017 (diamond).

Pablo and San Francisco. Water depth in the Delta varies from a few meters in shallow flooded islands to 13 m in the center of major river channels. Tides reach 2 m in height, have velocities up to 30 cm s^{-1} and range 10 km during tidal excursion. Due to its Mediterranean, climate summers are dry, and the water year is based on precipitation from October to the following September (Swain et al., 2018). *Microcystis* blooms commonly occur during the summer between July and October and were first observed in the Delta during the fall of 1999.

3. Methods

3.1. Field sampling

Data were obtained from two separate field studies conducted between July and November within the Delta at 10 stations in both 2014 and 2017. Both studies sampled stations across the USFE, with six of the stations sampled in both years (Table 1). Stations which were in close proximity and sampled in only one of the years were combined for spatial comparisons. Stations 4 and 5 and stations 8 and 9 were renamed for analysis as stations 5 and 9, respectively. Combining these stations enabled comparison of 8 locations across the two years. Sampling frequency differed between years, with samples collected every 2-weeks in 2014 and every 4-weeks in 2017. Water samples were collected with a van Dorn bottle (0.3 m in 2014) or from a through-hull boat pumping system (1 m in 2017) and were immediately stored at 4 °C for processing within 1–3 h.

Water temperature, pH, specific conductance, turbidity (NTU), and dissolved oxygen concentration were measured within the first 1 m using a Yellow Springs Instrument (YSI) 6600 water quality sonde.

Surface *Microcystis* colonies greater than 75 μm in diameter were gently collected with a 0.3 m diameter plankton net (75 μm mesh) that was hand-towed up to 30.5 m. The net was fitted with floats that kept the ring just below the surface, making the net tow an integrated sample of the surface layer. The net was also fitted with a General Oceanics 2030R flow meter to allow calculation of the total volume sampled. A surface net tow was used to get a representative sample of the wide diameter (e.g., 50,000 μm diameter) *Microcystis* colonies, because colonies were widely dispersed across the surface of the water column. A wide mesh was also necessary to reduced clogging from the high suspended sediment concentration, which characterizes the Delta.

Table 1
Stations sampled during the *Microcystis* bloom season in 2014 and 2017 are marked with an "X". The location of each station by number is presented in Fig. 1.

station	description	2014	2017
1	Suisun Channel		X
2	Collinsville	X	X
3	Antioch	X	X
4	Sherman Island		X
5	Brannon Island	X	
6	Jersey Point	X	X
7	Franks Tract	X	X
8	Potato Slough		X
9	San Joaquin River	X	
10	Mokelumne River		X
11	Rough and Ready Island	X	X
12	Venice Cut	X	
13	Old River	X	X
14	Mildred Island	X	

3.2. Water quality

Water for chloride, ammonium, nitrate plus nitrite, silica and soluble reactive phosphorus (SRP) analysis was immediately filtered through nucleopore filters (0.45 μm pore size) and frozen until analysis (American Public Health Association et al., 1998; United States Environmental Protection Agency, 1983; United States Geological Survey, 1985). Water for dissolved organic carbon analysis was filtered through a pre-combusted GF/F filter (pore size 0.7 μm) and kept at 4 °C until analysis (American Public Health Association et al., 1998). Unfiltered water samples for total and volatile suspended solids, total organic carbon and total phosphate analyses were kept at 4 °C until analysis (American Public Health Association et al., 1998).

3.3. Phytoplankton and cyanobacteria composition

Net tow samples for determination of surface *Microcystis* biovolume (>75 μm diameter size fraction) were preserved with Lugol's solution. The biovolume of surface *Microcystis* colonies was determined using area based diameter (ABD) with a FlowCAM digital imaging flow cytometer (Fluid Imaging Technologies; Sieracki et al., 1998). To more easily measure the biovolume of the colonies, the samples were subdivided into <300 μm and >300 μm diameter size fractions and read at a magnification of 10X and 4X, respectively.

Phytoplankton and cyanobacteria cell count data were also obtained for five stations sampled by the California Department of Water Resources environmental monitoring program (water.ca.gov/Programs/Environmental-Services/Interagency-Ecological-Program/Data-Portal). For these samples, water was collected at 1-m depth and preserved with Lugol's solution in glass bottles. Identification and enumeration of taxa to genus were done at 800X with the inverted microscopic technique (Utermohl, 1958).

3.4. Quantitative polymerase chain reaction (qPCR) analysis

A qPCR analysis of water samples collected from 0.3 to 1 m depth was used to quantify the potentially toxic cyanobacteria in all size fractions within the water column. Water samples (200–300 ml) for qPCR analysis were filtered through nitrocellulose membrane filters (pore size 0.45 μm) and the filters were used for DNA extraction using a NucleoSpin Plant II Kit (Macherey-Nagel, Bethlehem, Pennsylvania). The qPCR assays were used to quantify the gene targets: 16S ribosomal RNA genes (16S rDNA) for *Dolichospermum*, *Aphanizomenon*, *Microcystis*, and total cyanobacteria (Lehman et al., 2017). The qPCR assay for total cyanobacteria was developed against the conserved region of three cyanobacterial genera: *Microcystis*, *Dolichospermum*, and *Nostoc*. The assay also reacts with a wide range of cyanobacteria including *Aphanizomenon*, *Planktothrix*, and *Cylindrospermum*. The copy numbers of 16S rDNA gene were divided by the number of 16S rDNA per genome to obtain the equivalent cell number: *Microcystis aeruginosa* (2 copies, GenBank accession number: AP009552.1), *Dolichospermum* (4 copies, CP003659.1), and *Aphanizomenon* (6 copies, NZ_AZYY00000000.1). For total cyanobacteria, the number of cell equivalents was calculated by dividing the 16S rDNA copy number by 2 because *Microcystis* was the dominant species in SFE (Lehman et al., 2005; Baxa et al., 2010).

3.5. Microcystin concentration

Microcystin concentration (microcystin-LR equivalents) in particulate (algal cells) and dissolved fractions (water) within water samples was determined using a protein phosphatase inhibition assay (PPIA) kit (Product No. 520032, ABRAXIS, Warminser, PA). Particulate and dissolved fractions were separated by filtering the whole water sample through a glass fiber membrane (934-AH, 0.45 μm pore size, Whatman). Particulate organic matter on the filter was subjected to microcystin extraction using 80% methanol, followed by dilution before quantification of microcystin in the algal fraction by PPIA. The filtrate was used directly for PPIA analysis.

4. Data analysis

Streamflow and agricultural diversion data were obtained from DAYFLOW (https://water.ca.gov/Programs/Environmental-Services/Compliance-Monitoring-And-Assessment/Dayflow-Data). Data were analyzed using nonparametric techniques using the statistical package PRIMER-e v. 7 (Clarke and Gorley, 2015). Single and multiple comparisons were computed using ANOSIM. Multivariate analysis was conducted with the DISTLM routine in combination with BEST and an adjusted R^2 criteria to identify and model significant variables associated with *Microcystis* abundance. Distance based redundancy analysis (dbRDA) was then used to develop an ordination with the fitted model variables. Before multivariate analyses variables with high intercorrelation ($r \geq 0.85$) were removed from the analyses. Summary values in the text are the mean and standard deviation. Multiple regression analyses were computed with R software (R Core Team, 2017).

5. Results

5.1. Hydrology

Average water year outflow reached a high of 1918 $m^3\ s^{-1}$ in 2017 compared with a low outflow of 167 $m^3\ s^{-1}$ in 2014 and was accompanied by extreme maximum and minimum monthly values of 7532 $m^3\ s^{-1}$ and 90 $m^3\ s^{-1}$ for 2017 and 2014, respectively (Fig. 2a). The extreme nature of these years becomes clearer in comparison with the average monthly outflow for 2000-2016, excluding 2014, of 512 ± 679 $m^3\ s^{-1}$ (range 5024 $m^3\ s^{-1}$ to 86 $m^3\ s^{-1}$), which was 3–4 times higher or lower than the average outflow for 2014 and 2017, respectively. During the *Microcystis* bloom season between July and November, the average outflow in 2017 of 287 ± 44 $m^3\ s^{-1}$ was over twice as high as that in 2014 of 112 ± 21 $m^3\ s^{-1}$ (Fig. 2b). Outflow reflects the combined streamflow from the Sacramento and San Joaquin Rivers, which is a good index of the relative streamflow for most streamflow metrics in the estuary developed for DAYFLOW. However, *Microcystis* is commonly more abundant in the San Joaquin River, where average streamflow during the bloom season increased by a factor of 9 from 13 ± 8 $m^3\ s^{-1}$ in 2014 to 116 ± 66 $m^3\ s^{-1}$ in 2017 (Table 2). Most of the outflow is generated from the Sacramento River, which increased by a factor of 3 from an average of 94 ± 14 $m^3\ s^{-1}$ in 2014 to 298 ± 54 $m^3\ s^{-1}$ in 2017 near Rio Vista. Outflow also influenced the residence time of the water in the upper estuary, which is characterized by the X2 index. The X2 index describes the distance from the mouth of the estuary to the location landward where the bottom salinity is 2 (Jassby et al., 1995). The average X2 index for the 2017 water year (64 ± 15 km) was the lowest on record since 2000, indicating an extremely short residence time for water upstream, and was accompanied by a low monthly index value of 44 km in February and March (Fig. 2c). During the *Microcystis* bloom season, the X2 index in 2017 remained below 80 km and averaged 75 ± 2 km (Fig. 2d). The X2 index for 2014 (84 ± 4 km) was the highest index on record since 2000, suggesting dry conditions produced a long water residence time upstream due to the saltwater intrusion (Fig. 2c) and the average was slightly higher (87 ± 2 km) over the bloom season (Fig. 2d). The X2 index during the bloom season in 2014 was significantly different from 2017 and remained above 85 km; the highest index was at 89 km in September and October.

5.2. Bloom magnitude and distribution

Average surface biovolume for the same 8 locations measured between July and November was nearly 6 orders of magnitude (log values) greater in 2014 than 2017 ($p < 0.01$; Fig. 3a). The two orders of magnitude greater abundance of *Microcystis* in the subsurface water between 2014 and 2017 was also significant ($p < 0.01$).

The total microcystins concentration in the subsurface water was also significantly greater in 2014 than 2017. Average total microcystin concentration was 1.1 ± 3.8 μg L^{-1} in 2014 and decreased by 7 times in 2017 to 0.16 ± 0.20 μg L^{-1} (Fig. 3b). Toxin concentrations were greater in July through September compared with October and November for both years ($p < 0.05$). Variability was high and there were no significant differences in the mean among stations. However, the average concentration was elevated at Brannon Is. (station 5) in 2014 and Old River (station 13) in 2017 (not shown).

Surface *Microcystis* biovolume was significantly different for all months between July and November in 2014 and decreased by 3 orders of magnitude from a peak near 10 log $\mu m^3\ L^{-1}$ in July to 7 log $\mu m^3\ L^{-1}$ in November (Fig. 4a). Surface *Microcystis* biovolume peaked later in the

Table 2
Monthly mean and standard deviation for environmental variables measured during the *Microcystis* bloom season from July through November in 2014 and 2017. Measurements were based on samples collected at 2-week intervals for 2014 and 4-week intervals for 2017 at 8 common stations. Differences between months or between years were either significant at the 0.01 (**) level or were non-significant (ns).

	2014						2017					
Variable	July	August	September	October	November	month	July	August	September	October	November	month	year
outflow at confluence, $m^3\ s^{-1}$	118 ± 6	97 ± 10	100 ± 3	128 ± 32	133 ± 5	**	198 ± 8	275 ± 3	390 ± 3	288 ± 9	248 ± 7	**	**
X2 index, km	86 ± 0.1	88 ± 1	89 ± 0	88 ± 1	85 ± 1	**	71 ± 1	77 ± 1	75 ± 1	74 ± 1	77 ± 1	**	**
Sacramento River at Rio Vista, $m^3\ s^{-1}$	108 ± 8	95 ± 11	95 ± 9	70 ± 19	102 ± 25	**	225 ± 33	311 ± 22	375 ± 47	291 ± 70	286 ± 63	**	**
San Joaquin River at Vernalis, $m^3\ s^{-1}$	8 ± 1	8 ± 1	9 ± 1	15 ± 10	27 ± 10	**	224 ± 84	132 ± 10	90 ± 21	77 ± 12	58 ± 16	**	**
water temperature, °C	24.0 ± 1.4	23.2 ± 1.9	22.01 ± 0.7	20.08 ± 1.4	15.9 ± 1.5	**	23.6 ± 1	22.9 ± 1.0	23.3 ± 0.7	17.7 ± 0.5	15.2 ± 0.4	**	ns
dissolved oxygen, $mg\ L^{-1}$	7.7 ± 0.9	7.9 ± 0.6	8.4 ± 8.3	8.3 ± 0.6	8.6 ± 0.4	**	8.5 ± 0.5	8.1 ± 0.6	7.9 ± 0.1	8.8 ± 0.4	8.8 ± 0.3	**	ns
specific conductance, $\mu S\ cm^{-1}$	1924 ± 2112	1998 ± 1953	2676 ± 422	3415 ± 3562	2689 ± 2856	ns	310 ± 402	620 ± 915	384 ± 422	456 ± 590	1082 ± 1917	ns	**
turbidity, NTU	8.6 ± 5.8	8.2 ± 5.1	9.1 ± 5.8	5.4 ± 4.1	7.03 ± 5.7	ns	12.2 ± 7.0	8.1 ± 4.0	7.9 ± 5.8	10.2 ± 9.3	6.4 ± 5.0	ns	ns
pH	7.9 ± 0.3	8.0 ± 0.2	8.0 ± 0.2	7.7 ± 0.3	7.6 ± 0.1	**	7.6 ± 0.3	7.7 ± 0.1	7.5 ± 0.2	7.4 ± 0.2	7.4 ± 0.1	**	**
ammonium, $mg\ L^{-1}$	0.02 ± .02	0.02 ± 0.01	0.03 ± 0.03	0.05 ± 0.04	0.07 ± 0.04	**	0.04 ± 0.03	0.05 ± 0.03	0.07 ± 0.03	0.07 ± 0.03	0.08 ± 0.03	ns	**
nitrate, $mg\ L^{-1}$	0.33 ± 0.33	0.36 ± 0.40	0.44 ± 0.29	0.63 ± 0.81	0.58 ± 0.35	**	2.02 ± 5.33	0.25 ± 0.12	0.34 ± 0.29	0.42 ± 0.61	0.54 ± 0.33	**	ns
dissolved oxygen, $mg\ L^{-1}$	2.9 ± 0.74	3.2 ± 0.89	2.77 ± 0.27	2.75 ± 0.81	2.44 ± 0.52	**	2.69 ± 0.24	2.15 ± 0.24	2.11 ± 0.27	2 ± 0.44	2.16 ± 0.47	**	ns
total organic carbon, $mg\ L^{-1}$	3.1 ± 0.8	3.2 ± 1.0	2.92 ± 0.28	2.8 ± 0.8	2.52 ± 0.50	**	2.65 ± 0.26	2.19 ± 0.25	2.15 ± 0.28	2.01 ± 0.44	2.29 ± 0.38	**	**
dissolved organic nitrogen, $mg\ L^{-1}$	0.38 ± 0.11	0.39 ± 0.35	0.34 ± 0.11	0.26 ± 0.12	0.13 ± 0.11	**	0.18 ± 0.12	0.19 ± 0.11	0.1 ± 0.11	0.15 ± 0.11	0.19 ± 0.06	ns	**
soluble reactive phosphorus, $mg\ L^{-1}$	0.12 ± 0.09	0.12 ± 0.12	0.14 ± 0.03	0.14 ± 0.12	0.09 ± 0.03	**	0.06 ± 0.03	0.08 ± 0.02	0.08 ± 0.03	0.08 ± 0.08	0.07 ± 0.02	**	**
total phosphate, $mg\ L^{-1}$	0.16 ± 0.12	0.16 ± 0.14	0.17 ± 0.03	0.24 ± 0.45	0.10 ± 0.03	**	0.08 ± 0.02	0.08 ± 0.02	0.08 ± 0.03	0.09 ± 0.08	0.08 ± 0.03	ns	**
silica, $mg\ L^{-1}$	12.2 ± 2.0	13.4 ± 1.3	14.48 ± 1.9	15.5 ± 1.3	17.07 ± 1.4	**	5.8 ± 2.5	11.16 ± 1.8	14.88 ± 1.9	14.24 ± 1.4	14.52 ± 0.90	**	**
volatile suspended solids, $mg\ L^{-1}$	2.1 ± 1.2	2.1 ± 1.0	1.8 ± 1.5	1.9 ± 1.1	1.6 ± 1.3	ns	3 ± 1.7	1.75 ± 1.3	1.62 ± 1.5	1.88 ± 2.2	1 ± 0.90	ns	ns
total dissolved solids, $mg\ L^{-1}$	1774 ± 3394	1137 ± 1094	1498 ± 1936	1936 ± 2043	1484 ± 1607	ns	171 ± 223	215 ± 171	213 ± 230	254 ± 319	664 ± 1259	ns	**
total suspended solids, $mg\ L^{-1}$	9.9 ± 7.4	10.9 ± 7.3	9.9 ± 7.8	7.8 ± 4.9	8.6 ± 5.4	ns	18.5 ± 10.4	9.9 ± 7.3	9.9 ± 8.2	15.9 ± 19.6	7 ± 4.5	ns	ns

season for 2017 during September and October and the decrease from high to low values was greater than in 2014; 5 orders of magnitude between the peak value near 7 log $\mu m^3\ L^{-1}$ and the low value near 2 log $\mu m^3\ L^{-1}$. Subsurface abundance was consistently high early in the season between July and September for 2014 and again was greater later in the season during September for 2017 ($p < 0.05$; Fig. 4b).

Microcystis surface biovolume was highly variable across the Delta and was not significantly different among stations over the season for either 2014 or 2017 (Fig. 4c). However, surface biovolume tended to be greater in 2014 within the south Delta near Rough and Ready Is. (station 11) and upstream of the confluence near Brannon Is. (station 5), while in 2017 surface biovolume was elevated in the central Delta near Jersey Point (station 6), Franks Tract (station 7) and Old River (station 13). Subsurface abundance was also greater landward in 2014, with greater *Microcystis* abundance in the southern Delta at Rough and Ready Is. (station 11) than other stations ($p < 0.05$; Fig. 4d). In 2017, subsurface abundance was located more seaward than in 2014, with greater *Microcystis* abundance near Old River (station 13) in the central Delta than stations either further landward in the San Joaquin River (station 9) and Rough and Ready Is. (station 11) or seaward near Brannon Is. (station 5; $p < 0.05$).

5.3. Primary producer composition

Other cyanobacteria in the subsurface water comprised a greater percentage of the total cyanobacteria abundance in 2014 (69%) than 2017 (97%; $p < 0.01$; Fig. 5a and b). The most abundant of these other cyanobacteria was the small (~1 μm diameter) *Chroococcus microscopicus,* which aggregate into large colonies in the freshwater regions of the estuary and dominated the percent carbon of all primary producers for both years (not shown). Among the three potentially toxic cyanobacteria measured, *Microcystis, Aphanizomenon* and *Dolichospermum*, *Microcystis* cells comprised the largest percentage of the total cyanobacteria abundance in both 2014 and 2017, and the percentage decreased by a factor of 16 from 24% in 2014 to 1.5% in 2017 ($p < 0.01$; Fig. 5a and b). A similar decrease in the percent abundance of *Aphanizomenon* cells occurred between 2014 (8%) and 2017 (<1%; $p < 0.01$). The percentage of *Dolichospermum* cells remained below 2% in both years.

Among eukaryotic phytoplankton, cryptophytes were more abundant than diatoms and green algae in 2014 ($p < 0.01$; Fig. 5c). In 2017, green algae were more abundant than diatoms and cryptophytes (Fig. 5d; $p < 0.01$). Over the bloom season, high variability precluded significant differences among months, but cryptophytes (particularly *Plagioselmis nannoplanctica*) were relatively common in July and August of 2014, while the diatoms *Aulacoseira* spp. (seaward) and *Cyclotella* spp. (landward) were common in July 2017.

5.4. Environmental factors

Lower outflow and longer residence time in the upper estuary characterized 2014 compared with 2017 (Table 2). High outflow probably contributed to the lower specific conductance, total dissolved solids concentration and pH and the higher dissolved oxygen concentration over the season in 2017 compared with 2014. The high outflow in 2017 was also associated with lower nutrient concentrations for soluble reactive phosphorus, total phosphate, and silica by as much as a factor of 2 compared with 2014. Only ammonium and nitrate concentration were greater in 2017 than 2014. The *Microcystis* bloom in 2017 was also associated with lower dissolved and total organic carbon and dissolved organic nitrogen compared with 2014. The high outflow in 2017, however, was not associated with a reduction in seasonal average water temperature. Within each year, most variables differed among some months, with only outflow and the X2 index differing for all months. In contrast, ammonium concentration, dissolved organic nitrogen and total phosphate did not differ among months in 2017 (Table 2).

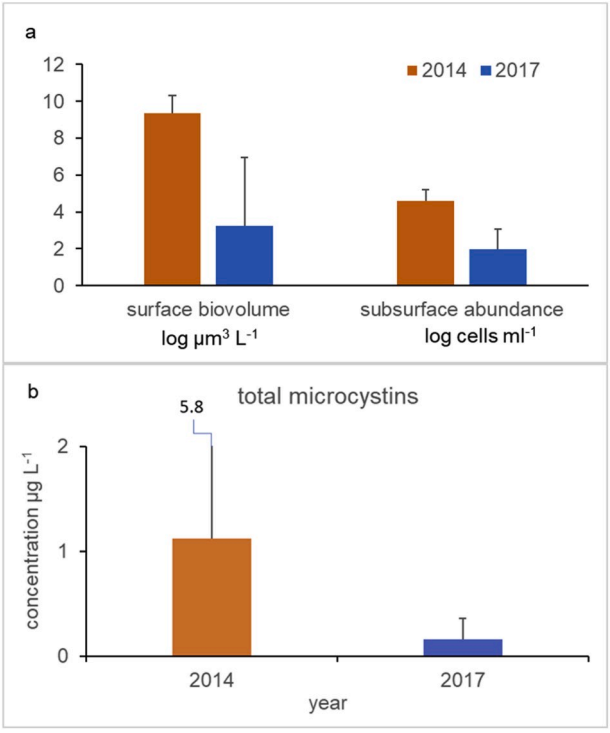

Fig. 3. Seasonal average log surface biovolume and log subsurface abundance (a) and total microcystins concentration (b) measured for *Microcystis* blooms in 2014 (orange) and 2017 (blue) at 8 locations sampled in both years. (For interpretation of the references to colour in this figure legend, the reader is referred to the Web version of this article.)

DISTLM analysis identified the X2 index, water temperature, ammonium concentration and silicate concentration as variables that described most of the variation (adj. $R^2 = 0.48$) in *Microcystis* surface biovolume in 2014 and 2017. Somewhat more of the variation in subsurface *Microcystis* abundance was described with the X2 index, water temperature, ammonium and pH concentration (adj. $R^2 = 0.70$).

The major patterns in the fitted model for the subsurface abundance data were demonstrated by a dbRDA ordination, which accounted for a majority (95%) of the fitted dbRDA variation and 67% of the total variation along the x-axis (Fig. 6). The strong correlation of *Microcystis* abundance with the X2 index and water temperature was demonstrated by the increase in *Microcystis* subsurface abundance (bubble size) horizontally along the X2 vector (X2 index) and vertically along the WT vector (water temperature). The stronger influence of these variables during the 2014 dry year compared with the 2017 wet year is suggested by the positioning of the 2014 abundance data farther away from the center of the circle than for 2017.

A 3D scatter plot in Fig. 7 demonstrates the threshold response of *Microcystis* subsurface abundance with respect to the X2 index and water temperature. *Microcystis* subsurface abundance and surface biovolume (not shown) were highest in 2014 when the X2 index was above 85 km and the water temperature was 25 °C. Peak *Microcystis* subsurface abundance also occurred at 25 °C in 2017, but the overall abundance was less than 2014 due to the relatively lower X2 index, which was less than 80 km. The importance of the X2 index as a threshold for controlling *Microcystis* bloom magnitude was further demonstrated by correlation analysis. *Microcystis* subsurface abundance was linearly correlated with the X2 index ($r = 0.79$, $p < 0.01$) for both years combined, but the correlation was not significant within either 2014 ($r = 0.211$, $p > 0.05$) or 2017 ($r = 0.01$, $p > 0.05$) separately. In contrast, *Microcystis* subsurface abundance consistently increased with water temperature for both years combined ($r = 0.45$, $p < 0.01$), as well as for 2014 ($r = 0.80$, $p < 0.01$) and 2017 ($r = 0.38$, $p < 0.01$) separately. Using multiple regression models, it was possible to predict a significant

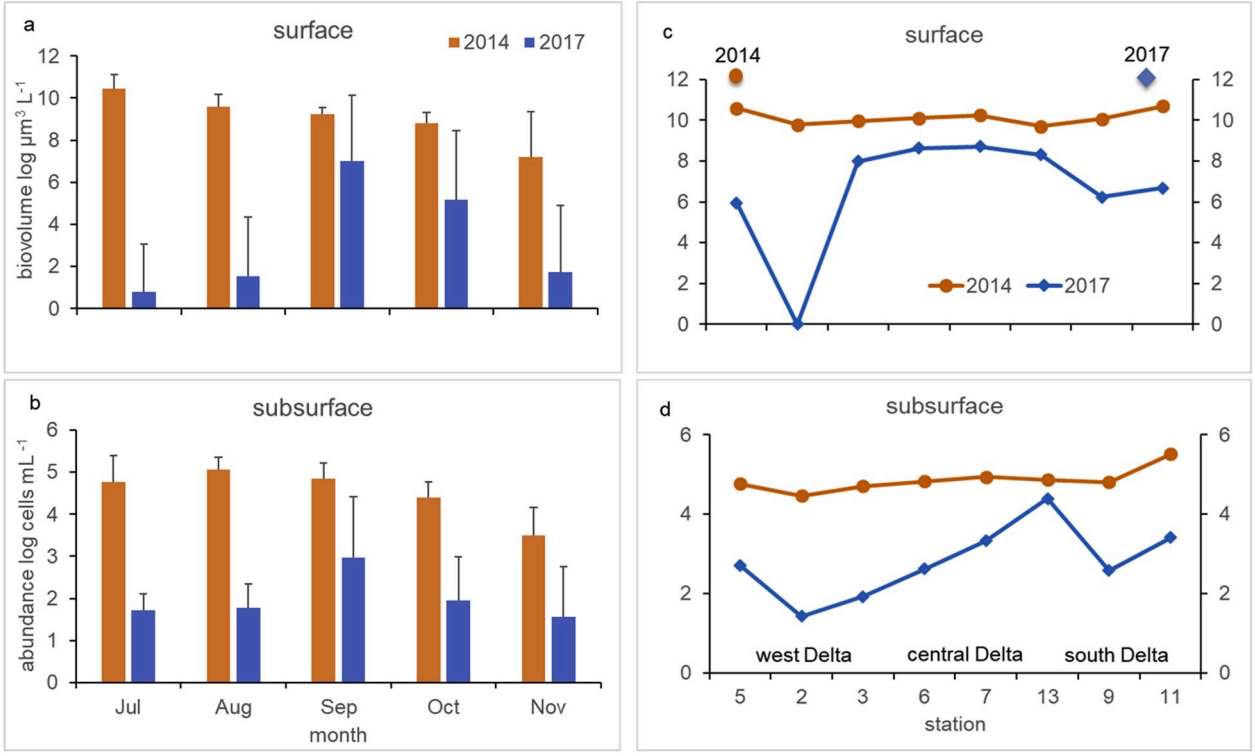

Fig. 4. Monthly average log surface biovolume (a) and log subsurface abundance (b) of *Microcystis* colonies sampled during the bloom season and the average log surface biovolume (c) and log subsurface abundance (d) of *Microcystis* colonies measured among stations for 2014 (orange, circle) and 2017 (blue, diamond). (For interpretation of the references to colour in this figure legend, the reader is referred to the Web version of this article.)

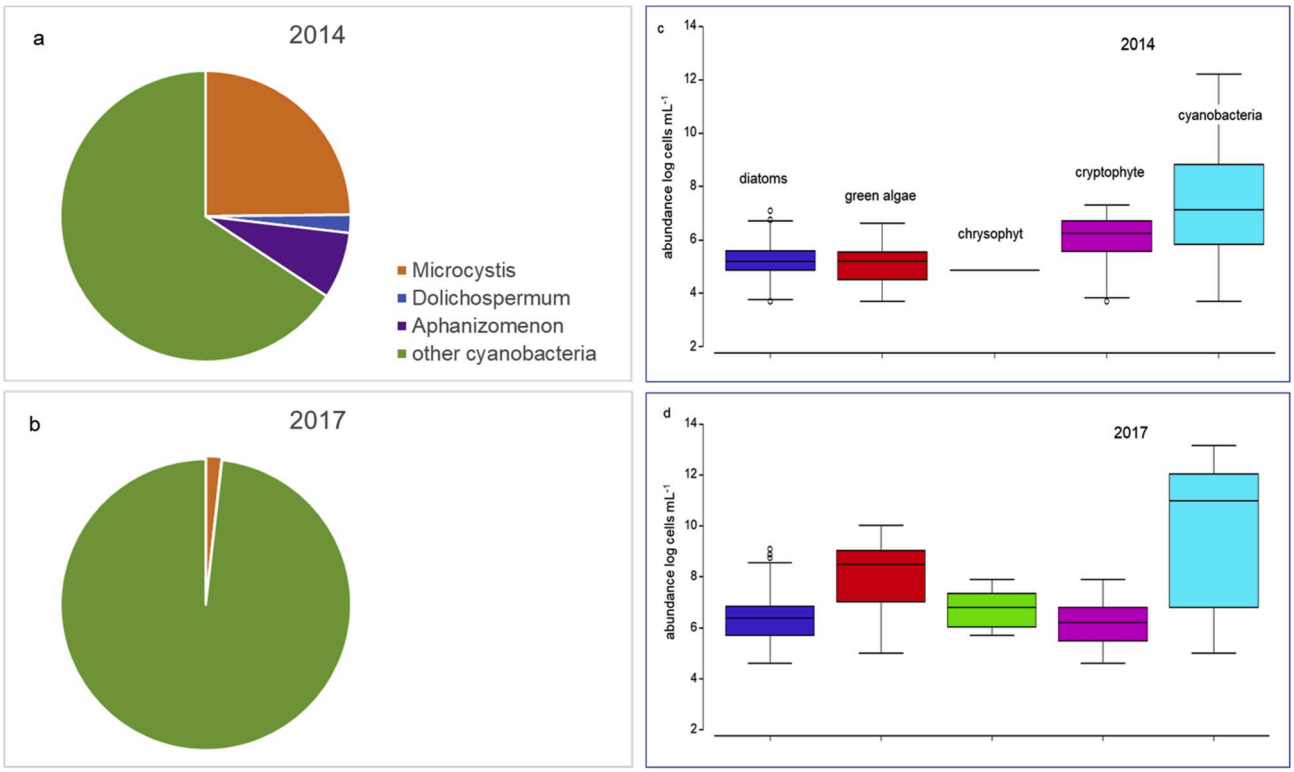

Fig. 5. Pie charts describing the relative percent abundance of cyanobacteria taxa measured by qPCR analysis for 2014 (a) and 2017 (b) and box plots indicating the median, 1st and 3rd quartiles, maximum and minimum log abundance of 5 phytoplankton taxa measured microscopically for 2014 (c) and 2017 (d). All computations were conducted for subsurface samples collected during the *Microcystis* bloom season between July and November at 8 locations.

proportion of the variation in the log of *Microcystis* surface biovolume (adj. $R^2 = 0.78$) and subsurface abundance (adj. $R^2 = 0.58$) with the X2 index and water temperature (Table 3). Interaction terms were not significant. Addition of ammonium and silicate (surface biovolume) or ammonium and pH (subsurface abundance; Fig. 6) did not add significantly to the description of variance in the regression analysis.

6. Discussion

It was not unexpected that the X2 index would account for most of the variation in the *Microcystis* bloom abundance in USFE. Streamflow variables have been identified as critical factors controlling the magnitude of *Microcystis* blooms worldwide (Paerl and Otten, 2013) and in USFE (Lehman et al., 2008). Although nutrient concentration, especially nitrogen and phosphorus are commonly critical controlling factors for *Microcystis* growth (Harke et al., 2016), streamflow would be expected to be more important in USFE, where nutrient concentrations are in excess (Jassby, 2008). The unexpected persistence of *Microcystis* during the extreme wet conditions of 2017, caused us to reject the hypothesis that an extreme wet year would prevent bloom formation and perhaps return the estuary to pre-bloom conditions. Previous research suggested that *Microcystis* blooms occurred when the average streamflow was below 80 $m^3 s^{-1}$ in the upper San Joaquin River and below 300 $m^3 s^{-1}$ in the lower Sacramento River near Rio Vista (Lehman et al., 2013). These values were well below the average streamflow of 90 $m^3 s^{-1}$ in the San Joaquin River and 373 $m^3 s^{-1}$ in the Sacramento River near Rio Vista measured during September 2017, when *Microcystis* was most abundant. That a *Microcystis* bloom could persist during wet year conditions in USFE was supported by data collected in 2011 when *Microcystis* abundance peaked at the end of the bloom season in October (Mioni et al., 2011), when seasonal average outflow was 331 $m^3 s^{-1}$ (Fig. 2a).

The importance of the X2 index threshold in predicting the amplitude of the *Microcystis* bloom supports the importance of residence time

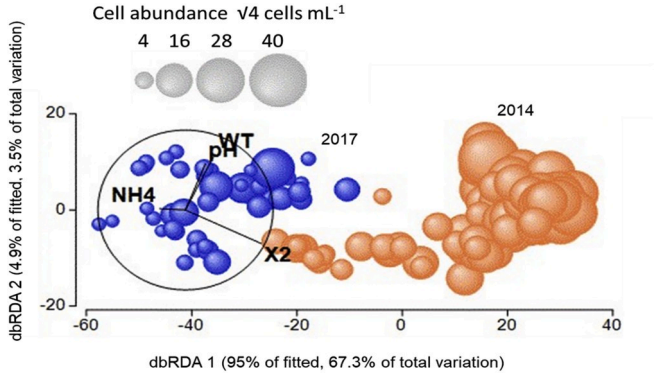

Fig. 6. Redundancy analysis (dbRDA) ordination computed using DISTLM (PRIMER) for *Microcystis* subsurface abundance ($\sqrt{4}$ cells mL^{-1}) and the environmental variables X2 index (X2), water temperature (WT), pH (pH) and ammonium (NH4) that described a significant proportion of the data variation for all samples collected between July and November of 2014 (orange spheres) and 2017 (blue spheres). The relative importance of each environmental variable is indicated by the vector length away from the circle center. The cell abundance is indicated by the size of the sphere. (For interpretation of the references to colour in this figure legend, the reader is referred to the Web version of this article.)

thresholds for bloom development in USFE. The *Microcystis* bloom in USFE reached peak levels when the X2 index was above 85 km, upstream of Antioch at the western edge of the Delta. A salt wedge at this location would impede the movement of colonies seaward out of the Delta. *Microcystis* blooms are often more dependent on the accumulation of colonies rather than growth, because *Microcystis* has a slow growth rate compared with eukaryotes (Paerl and Otten, 2013; Lehman et al., 2008). Streamflow thresholds are often considered to be important controls for

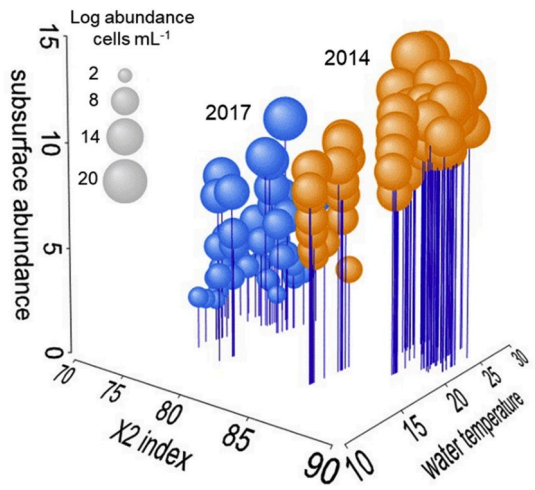

Fig. 7. Association between *Microcystis* abundance (log cells mL^{-1}) for all samples measured in the subsurface water on the Y axis (spheres) with the environmental variables X2 index (km) on the X axis and water temperature (°C) on the Z axis for 2014 (orange spheres) and 2017 (blue spheres). . (For interpretation of the references to colour in this figure legend, the reader is referred to the Web version of this article.)

cyanobacteria blooms in estuaries and lakes. An upper streamflow threshold was suggested to control bloom development in the Neuse River estuary of 15 $m^3 s^{-1}$ (Christian et al., 1986; Yang et al., 2018) and of 75 $m^3 s^{-1}$ for *Microcystis* in Lake Volkerak in the Scheldt Estuary, The Netherlands (Verspagen et al., 2006). Similarly, streamflow threshold values based on sustained streamflow (3.5 $m^3 s^{-1}$) and flushing flows (35 $m^3 s^{-1}$) were proposed to control *Dolichospermum* blooms in the Lower Darling Reservoir, Australia (Mitrovic et al., 2011). Importantly, relatively small changes in the location of the X2 index may be important. A shift of the X2 index by only 3 km was associated with a factor of 3 increase in the percent abundance of subsurface *Microcystis* cells in the cyanobacterial community between the extreme drought years 2014 and 2015 (Lehman et al., 2018). Similarly, the increase in the X2 index from 71 km in July to between 75 and 76 km in August and September may have facilitated retention of cells in the central Delta during the peak of the bloom in 2017.

Water temperature is often identified as a significant factor controlling *Microcystis* blooms (Jiang et al., 2008) and has previously been identified as a strong correlate for blooms in USFE (Lehman et al., 2008). The water temperature threshold during the bloom seasons in 2014 and 2017 were above the 19 °C threshold for bloom initiation in USFE (Lehman et al., 2013), and optimum for bloom development (Paerl and Otten, 2013). However, increasing water temperature was also important once the threshold was exceeded, because *Microcystis* abundance and water temperature were positively correlated for both years. The lower average bloom magnitude in 2017 was partially due to the failure of water temperature to reach 25 °C as often as in 2014. The ability of *Microcystis* to increase with water temperature is thought to provide *Microcystis* with a competitive advantage over phytoplankton and other cyanobacteria when water temperature is above 20 °C (Huisman et al., 2018).

Regression analysis suggested the X2 index and water temperature were the primary factors controlling the *Microcystis* bloom during the two extreme water years, even though analysis suggested other environmental factors may have contributed to bloom development. The factor of 2 higher ammonium concentration in 2017 than 2014 could have favored *Microcystis* bloom growth but was probably not an important causal factor due to the negative correlation with *Microcystis* abundance. *Microcystis* has a high uptake rate (V_{max}) for ammonium and the efficient utilization of ammonium as a nitrogen source may enable *Microcystis* to outcompete other micro primary producers (Takamura et al., 1987; Lee et al., 2015). High ammonium uptake rate can favor *Microcystis* in USFE, even though nitrogen is in excess, because *Microcystis* increases with the percentage of ammonium in the total nitrogen pool (Lehman et al., 2015). The strong correlation between *Microcystis* and pH probably reflected the change in the hydrogen ion concentration in the water column from increased primary productivity. However, *Microcystis* grows best at pH between 7 and 9 and can outcompete *Scenedesmus*, a common genus in the Delta, at pH 7-9, particularly when water temperature is near 35 °C (Yang et al., 2018). The positive correlation between silicate and *Microcystis* may reflect the importance of freshwater habitat to bloom formation (Lehman et al., 2013).

Although not tested directly, the composition of the primary producer community may have contributed to the persistence of the *Microcystis* bloom in 2017. Cyanobacteria within the primary producer community, comprised over 90% and 80% of the cell abundance in 2014 and 2017, respectively. Other non-toxic cyanobacteria were also more abundant than toxic cyanobacteria in 2014 and 2017. Metagenomic analysis identified over 19 cyanobacterial genera at one station alone in 2014 (Kurobe et al., 2018a). Cyanobacteria can release allelopathic substances that suppress eukaryotic phytoplankton (Paerl and Otten, 2013) and toxins produced by *Microcystis* can inhibit the growth of primary producers through multiple metabolic pathways (Song et al., 2017; Sedmak and Elersek, 2006; Suikkanen et al., 2005). Similarly, a large *Microcystis* bloom was associated with a decrease in the microbial community (Otten et al., 2017). It is also possible that the presence of *Microcystis* since 1999 could have slowly preconditioned the environment to support *Microcystis* over other primary producers and added colonies as a seed source to the sediment.

The USFE is a complex estuarine landscape comprised of deep river channels, flooded islands, shallow wetlands and backwater sloughs (Moyle et al., 2010) that could retain *Microcystis* colonies as a seed source for the estuary. *Microcystis* vegetative cells are often retained in bottom sediments of shallow water habitats during the winter and seed blooms the following year (Verspagen et al., 2006). Backwater areas could also seed *Microcystis* cells throughout the USFE during the wet season, when shallow water habitats flood and particles are carried long distances (Sommer et al., 2008). Modeling studies demonstrated horizontal transport is an important mechanism for bloom formation in USFE (Lucas et al., 1999). However, net transport computations also demonstrated shallow wetlands can retain chlorophyll despite high

Table 3
Multiple linear regression equations and associated statistics computed for the dependent variables describing the *Microcystis* bloom amplitude as log surface biovolume or log subsurface abundance with the independent variables that described most of the variability in the bloom amplitude, the X2 index (km) and water temperature (°C). n = 159.

dependent variable	independent variable	estimate	standard error	t-statistic	significance level	adj. R^2
surface biovolume	intercept	−35.1	2.85	−12.29	<0.001	0.78
log $\mu m^3 L^{-1}$	X2 index	0.44	0.03	13.84	<0.001	
	water temperature	0.24	0.06	4.22	<0.001	
subsurface abundance	intercept	−16.1	0.85	−19.01	<0.001	0.58
log cells mL^{-1}	X2 index	0.19	0.01	20.29	<0.001	
	water temperature	0.17	0.02	10.27	<0.001	

advective (river) and dispersive (tidal) flow in USFE (Lehman et al., 2010). Abundance data supported the retention of *Microcystis* cells in the central Delta during 2017. Once transported into the main river channels, cells would be able to grow as long as water temperature or other water quality thresholds were met, as in 2017, when water temperature was above the 19 °C threshold. It is also possible that *Microcystis* cells persist in the sediments at the bottom of the deep main river channels (12 m), where streamflow is low compared with the surface (Dugdale et al., 2016), and rise into the water column as water temperature increases to threshold levels in USFE. In Lake Limmaren, Sweden, *Microcystis* recruitment from sediments occurred from both shallow and deep areas (Brunberg and Blomqvist, 2003). However, the percent recruitment of colonies from the surface sediment layer was 6 times greater for shallow (50%) than deep areas (8%). We concluded that since *Microcystis* blooms have become established in the estuary, they will persist despite flushing from extreme wet conditions and will develop once water quality conditions, particularly water temperature, become favorable.

Declaration of competing interest

The authors agree there is no conflict of interest with regard to this work.

Acknowledgements

Funding for this project was obtained from the California Department of Water Resources, the California Department of Fish and Wildlife Drought Response Program and a California Department of Fish and Wildlife Proposition 1 Grant. Field and laboratory assistance was provided by the California Department of Water Resources Division of Environmental Services, especially S. Lesmeister, M. Dempsey, E. Santos, N. van Ark, S. Waller, T. Hollingshead, R. Elkins, H. Fuller, M. Legro, A. Lopez, M. Martinez, A. Munguia, M. Ogaz, A. Tung, M. Xiong, E. Jeu, and R. Mulligan. Water quality analyses were conducted by the California Department of Water Resources Bryte Laboratory.

References

Acuña, S.C., Baxa, D., Teh, S.J., 2012a. Sublethal dietary effects of microcystin producing *Microcystis* on threadfin shad, *Dorosoma petenense*. Toxicon 60, 1191–1202.

Acuña, S.C., Deng, D.-F., Lehman, P.W., Teh, S.J., 2012b. Dietary effects of *Microcystis* on Sacramento splittail, *Pogonichthys macrolepidotus*. Aquat. Toxicol. 110–111, 1–8.

American Public Health Association, American Water Works Association, Water Environment Association, 1998. Standard Methods for the Examination of Water and Wastewater, twentieth ed. American Public Health Association, Washington, D.C., USA.

Baxa, D.V., Kurobe, T., Ger, K.A., Lehman, P.W., Teh, S.J., 2010. Estimating the abundance of toxic *Microcystis* in the san Francisco estuary using quantitative Q-PCR. Harmful Algae 9, 342–349.

Brunberg, A.-K., Blomqvist, P., 2003. Recruitment of *Microcystis* (Cyanophyceae) from lake sediments: the importance of littoral inocula. J. Phycol. 39, 58–63.

Cayan, D., Tyree, M., Dettinger, M., Hidalgo, M., Das, H.T., Maurer, P.E., Bromirski, Graham, N., Flick, R., 2009. Climate Change Scenarios and Sea Level Rise Estimates for the California 2009 Climate Change Scenarios Assessment. California Climate Change Center CEC-500-2009-014-D.

Christian, R., Bryant, W., Stanley, D., 1986. The relationship between river flow and *Microcystis aeruginosa* blooms in the Neuse River, North Carolina, Rep. No. 223. University of North Carolina Water Resources Research Institute, Raleigh, North Carolina.

Clarke, K.R., Gorley, R.N., 2015. PRIMER-e v.7: User Manual/Tutorial. PRIMER-E Ltd, Devon, United Kingdom.

Dettinger, M., Anderson, J., Anderson, M., Brown, L., Cayan, D., Maurer, E., 2016. Climate change and the delta. San Franc. Estuary Watershed Sci. 14 (3) https://doi.org/10.15447/sfews.2016v14iss2art5. Article 5.

Dugdale, R.C., Wilkerson, F.P., Parker, A.E., 2016. The effect of clam grazing on phytoplankton spring blooms in the low-salinity zone of the San Francisco Estuary: a modeling approach. Ecol. Model. 340, 1–16.

Ger, K.A., Teh, S.J., Goldman, C.R., 2009. Microcystin-LR toxicity on dominant copepods *Eurytemora affinis* and *Pseudodiaptomus forbesi* of the upper San Francisco Estuary. Sci. Total Environ. 407, 4852–4857.

Ger, K.A., Teh, S.J., Baxa, D.V., Lesmeister, S.H., Goldman, C.R., 2010. The effects of dietary *Microcystis* aeruginosa and microcystin on the copepods of the upper San Francisco Estuary. Freshw. Biol. 55, 1548–1559.

Harke, M.J., Steffen, M.M., Gobler, C.J., Otten, T.G., Wilhelm, S.W., Wood, S.A., Paerl, H. W., 2016. A review of the global ecology, genomics, and biogeography of the toxic cyano - bacterium, *Microcystis* spp. Harmful Algae 54, 4–20.

Huisman, J., Codd, G.A., Paerl, H.W., Ibelings, B.W., Verspagen, J.M.H., Visser, P.M., 2018. Cyanobacterial blooms. Nat. Rev. Microbiol. 16, 471–483.

Intergovernmental Panel on Climate Change (IPCC), 2014. In: Pachauri, R.K., Meyer, L. A. (Eds.), Climate Change 2014: Synthesis Report. IPCC, Geneva, Switzerland, p. 151.

Jassby, A.D., 2008. Phytoplankton in the Upper San Francisco Estuary, Recent biomass trends, their causes and their trophic significance. San Franc. Estuary Watershed Sci. 6 (1). Article 2.

Jassby, A.D., Kimmerer, W.J., Monismith, S.G., Armor, C., Cloern, J.E., Powell, T.M., Schubel, J.R., Venflinski, T.J., 1995. Isohaline position as a habitat indicator for estuarine populations. Ecol. Appl. 5, 272–289.

Jiang, Y., Ji, B., Wong, R.N.S., Wong, M.H., 2008. Statistical study on the effects of environmental factors on the growth and microcystins production of bloom-forming cyanobacterium-*Microcystis aeruginosa*. Harmful Algae 7, 127–136.

Jones, J., 2015. California's Most Significant Droughts, Comparing Historical and Recent Conditions. California Department of Water Resources, Sacramento, California, p. 126. http://bibpurl.oclc.org/web/74277.

Kurobe, T.K., Lehman, P.W., Hammock, B.G., Bolotaolo, M.B., Lesmeister, S., Teh, S.J., 2018a. Biodiversity of cyanobacteria and other aquatic microorganisms across a freshwater to brackish water gradient determined by shotgun metagenomic sequencing analysis in the San Francisco Estuary, USA. PLoS One 13 (9), e0203953.

Kurobe, T., Lehman, P.W., Haque, Md E., Sedda, T., Lesmeister, S., The, S., 2018b. Evaluation of water quality during successive severe drought years within *Microcystis* blooms using fish embryo toxicity tests for the San Francisco Estuary, California. Sci. Total Environ. 610–611, 1029–1037.

Lee, J., Parker, A.E., Wilkerson, F.P., Dugdale, R.C., 2015. Uptake and inhibition kinetics of nitrogen in *Microcystis* aeruginosa, Results from cultures and field assemblages collected in the San Francisco Bay Delta, CA. Harmful Algae 47, 126–140.

Lehman, P.W., Boyer, G., Hall, C., Waller, S., Gehrts, K., 2005. Distribution and toxicity of a new colonial *Microcystis aeruginosa* bloom in the San Francisco bay estuary, California. Hydrobiologia 541, 87–90.

Lehman, P.W., Boyer, G., Satchwell, M., Waller, S., 2008. The influence of environmental conditions on the seasonal variation of *Microcystis* abundance and microcystins concentration in San Francisco Estuary. Hydrobiologia 600, 187–204.

Lehman, P.W., Teh, S.J., Boyer, G.L., Nobriga, M., Bass, E., Hogle, C., 2010. Initial impacts of *Microcystis* on the aquatic food web in the san Francisco estuary. Hydrobiologia 637, 229–248.

Lehman, P.W., Marr, K., Boyer, G.L., Acuna, S., Teh, S.J., 2013. Long-term trends and causal factors associated with *Microcystis* abundance and toxicity in San Francisco Estuary and implications for climate change impacts. Hydrobiologia 718, 141–158.

Lehman, P.W., Kendall, C., Guerin, M.A., Young, M.B., Silva, S.R., Boyer, G.L., Teh, S.J., 2015. Characterization of the *Microcystis* bloom and its nitrogen supply in San Francisco Estuary using stable isotopes. Estuar. Coasts 38, 165–178.

Lehman, P.W., Kuobe, T., Lesmeister, S., Baxa, D., Tung, A., The, S.J., 2017. Impacts of the 2014 severe drought on the *Microcystis* bloom in san Francisco estuary. Harmful Algae 63, 94–108.

Lehman, P., Kurobe, T., Lesmeister, S., Lam, C., Tung, A., Xiong, M., Teh, S., 2018. Strong differences characterized *Microcystis* blooms between successive severe drought years in San Francisco Estuary, CA. Aquat. Microb. Ecol. 81, 293–299.

Lucas, L.V., Koseff, J.R., Monismith, S.G., Cloern, J.E., Thompson, J.K., 1999. Processes governing phytoplankton blooms in estuaries. II: the role of horizontal transport. Mar. Ecol. Prog. Ser. 187, 17–30.

Miller, M.A., Kudela, R.M., Mekebri, A., Crane, D., Oates, S.C., Tinker, M.T., Staedler, M., Miller, W.A., Toy-Choutka, S., Dominik, C., Hardin, D., Langlois, G., Murray, M., Ward, K., Jessup, D.A., 2010. Evidence for a novel marine harmful algal bloom, cyanotoxin (microcystin) transfer from land to sea otters. PLoS One 5, e12576.

Mioni, C., Kudela, R., Baxa, D., Sullivan, M., 2011. Harmful Cyanobacteria Blooms and Their Toxins in Clear Lake and the Sacramento-San Joaquin Delta (California). in: Report Prepared for Central Valley Regional Water Quality Control Board, pp. 1–100.

Mitrovic, S.M., Hardwick, L., Dorani, F., 2011. Use of flow management to mitigate cyanobacterial blooms in the Lower Darling River, Australia. J. Plankton Res. 33, 229–241.

Moyle, P., Bennett, W.A., Fleenor, W.E., Lund, J.R., 2010. Habitat variability and complexity in the upper san Francisco estuary. San Franc. Estuary Watershed Sci. 8 (3).

Otten, T.G., Paerl, H.W., Dreher, T.W., Kimmerer, W.J., Parker, A.E., 2017. The molecular ecology of Microcytis sp. blooms in the san Francisco estuary. Environ. Microbiol. https://doi.org/10.1111/1462-2920.13860.

Paerl, H.W., Otten, T.G., 2013. Harmful cyanobacterial blooms, causes, consequences, and controls. Microb. Ecol. 65, 995–1010.

R Core Team, 2017. R: A Language and Environment for Statistical Computing. R Foundation for Statistical Computing, Vienna, Austria. URL. https://www.R-project.org/.

Robson, B.J., Hamilton, D.P., 2003. Summer flow event induces a cyanobacterial bloom in a seasonal Western Australia estuary. Mar. Freshw. Res. 54, 139–151.

Rocha, C., Galvão, H., Barbosa, A., 2002. Role of transient silicon limitation in the development of cyanobacteria blooms in the Guadiana estuary, south-western Iberia. Mar. Ecol. Prog. Ser. 228, 35–45.

Sedmak, B., Eleršek, T., 2006. Microcystins induce morphological and physiological changes in selected representative phytoplankton. Microb. Ecol. 5, 508–515.

Sellner, K.G., Lacouture, R.V., Parlish, K.G., 1988. Effect of increasing salinity on a cyanobacteria bloom in the Potomac River Estuary. J. Plankton Res. 10, 49–61.

Sieracki, C.K., Sieracki, M.E., Yentsch, C.S., 1998. An imaging-in-flow system for automated analysis of marine microplankton. Mar. Ecol. Prog. Ser. 168, 285–296.
Sommer, T.R., Harrell, W.C., Swift, T.J., 2008. Extreme hydrologic banding in a large-river floodplain, California, USA. Hydrobiologia 598, 409–415.
Song, H., Lavoie, M., Fan, S., Tan, H., Liu, G., Xu, P., Fu, Z., Paerl, H.W., Qian, H., 2017. Allelopathic interactions of linoleic acid andnitric oxide increase the competitive ability of *Microcystis* aeruginosa. ISME J. 11, 1865–1876.
Suikkanen, S., Fistarol, G.O., Granéli, E., 2005. Effects of cyanobacterial allelochemicals on a natural plankton community. Mar. Ecol. Prog. Ser. 287, 1–9.
Swain, D.L., Langenbrunner, B., Neelin, J.D., Hall, A., 2018. Increasing precipitation volatility in twenty-first-century California. Nat. Clim. Chang. 8, 427–433. https://doi.org/10.1038/s41558-018-0140-y://doi.org/10.1038/s41558-018-0140-ys://doi.org/10.1038/s41558-018-0140-y.
Takamura, N., Iwakuma, T., Yasuno, M., 1987. Uptake of 13C and 15N (ammonium, nitrate and urea) by *Microcystis* in Lake Kasumigaura. J. Plankton Res. 9 (1), 151–165.
United States Environmental Protection Agency, 1983. Methods for Chemical Analysis of Water and Wastes. United States Environmental Protection Agency, Washington, DC, USA. Technical Report EPA-600/4-79-020.
United States Geological Survey, 1985. Methods for determination of inorganic substances in water and fluvial sediments. Open File Rep. 85–495.
Utermohl, H., 1958. Zur Vervollkommung der quantitativen Phytoplankton-methodik. Mitteilumgen Internationale Verejunigung fur Theoretische und Angewandtet Limnologie 9, 1–38.
Verspagen, J.M.H., Passarge, J., Jöhnk, K.D., Visser, P.M., Peperzak, L., Boers, P., Laanbroek, H.J., Huisman, J., 2006. Water management strategies against toxic *Microcystis* blooms in the Dutch delta. Ecol. Appl. 16, 313–327.
Yang, J., Tang, H., Zhang, X., Zhu, X., Huang, Y., Yang, Z., 2018. High temperature and pH favor *Microcystis aeruginosa* to outcompete *Scenedesmus obliquus*. Environ. Sci. Pollut. Res. 25 (5), 4794–4802.
Yunes, J.S., Salomon, P.S., Matthiensen, A., Beattie, K.A., Raggett, S.L., Codd, G.A., 1996. Toxic blooms of cyanobacteria in the Patos Lagoon estuary, southern Brazil. J. Aquat. Ecosyst. Health 5, 223–229.